

Computer Aided Diagnosis Based on an Advanced FCN Segmentation Technique for Automating Prostate Region Delineation

¹Afef LATRACH, ¹Lamia SELLAMI, ¹Rania TRIGUI, ¹Ahmed BEN HAMIDA

²Mohamed FOURATI, ²Kaireddine BEN MAHFOUDH

¹ATMS Lab, Advanced Technologies for Medicine and Signals, ENIS, Sfax University, Sfax, Tunisia.

²University hospital Habib Bourguiba Sfax

Abstract - Computer Aided Diagnosis ‘CAD’ has become useful nowadays for helping physicians during pathology exploring. In this article, a CAD tool using an advanced segmentation technique of the various MRI slices in the T2 modality was done in order to explore prostate region. The idea behind was, in fact, to segment more efficiently the region of interest ‘ROI’ of the prostate. This will help considerably and more efficiently prostate clinical exploring and hence respond to several useful clinical needs.

Our proposed methodology could be henceforth as a first step the preprocessing phase that was based on an advanced denoising technique. We explore an anisotropic diffusion filter that could be enriched by a normalization and a histogram equalization phase ‘AHE’ through Contrast Limited Adaptive Histogram Equalization ‘CLAHE’ method. Such proposed preprocessing phase was consequently useful because the targeted segmentation process was considerably improved.

During the proposed segmentation technique of the MRI slices, we used a Deep Learning model referred to as Fully Connected Neural Network ‘FCN’. As an originality, this model was carefully modified by adding other residual connections in order to reinforce its efficiency. Such a modification reinforced the segmentation technique and this was by the highest accuracy value around 98 %.

Experimental results for various pathology cases represent at presenta useful CAD System that could be furnished to physicians during their exploring. Our proposed advanced MRI segmentation process could be extended henceforth towards a real aided tool dedicated to clinical prostate exploration.

Keywords: Computer aided diagnosis, Prostate exploring, ROI, Advanced segmentation, Modified FCN Model.

I. INTRODUCTION

Today's medicine has known an important turning point thanks to the progress made in medical imaging in its various forms, allowing an indirect visualization of the anatomy, physiology or metabolism of the human body. Magnetic Resonance Imaging (MRI) has become an essential technique in the exploration of body tissues. It represents a very useful imaging when a very fine analysis is needed and certain lesions are not visible on standard radiographs. MRI is widely used for diagnostic and therapeutic purposes. It is particularly advantageous for the diagnosis and treatment of prostate pathology by allowing the visualization and localization of suspicious lesions. Thus, it promotes the targeted biopsy and therapy. These latest applications require a precise segmentation, slice by slice [1].

Usually, physicians and radiologists exploited their visual capacity with scientific knowledge to analyze medical images for exploring several pathologies. This was in fact insufficient in major situations especially when the images involve several hesitations, or with a remarkable variability between slices or with big data. Nowadays, research involving medical image focus on quality improving and mainly on automatization task in order to provide clinical aided tools piloted by advanced algorithms [1, 2]

Clinically, several essential parameters are used as the prostate volume which helps in the evaluation of the prostate-specific antigen (PSA) density and could be used to determine treatment options as well as to quantify the treatment response. Such parameters were in fact important especially when analyzing MR imaging is a subjective and time-consuming task [3].

More than 30 MRI slices in the T2-W modality could be obtained usually for every MRI exam, and radiologists had to evaluate, carefully and individually, each slice. Because of the variation in prostate characteristics as in size and shape, sometimes, it would be so difficult to examine the cancer location from the vicinity tissues. The main objective

was in fact the determination of the ROI with the maximum precision which is henceforth so important for the following clinical action to be taken [3,4].

Prostate segmentation methods can be grouped into four groups according to the information used to guide the segmentation. These groups include contour and shape-based methods [3], region-based methods [4], supervised and un-supervised classification methods [5] and hybrid methods [5].

Prostatic volume extraction helps in the planning of biopsies, focal ablative, surgeries, radiation, etc... MRI allows calculating prostatic volume, but the shape of the prostate varies and the determination of its volume requires experiences and highly operator-dependent. For this reason, an automatic and operator-independent target delineation method is mandatory.

Consequently, our research would be focused on an automated and especially accurate segmentation technique for localizing prostate region within MR images in the T2 modality, offering then a computer aided tool helping to carefully identify the ROI.

Recently, Machine Learning area 'ML'[6] and Deep Learning 'DL'[7] have seen exponential progress and where massively used especially in MRI segmentation. These Techniques have produced models that present remarkable performances through many benchmark datasets [8].

Artificial intelligence method, in general learns from examples to make predictions without prior specific programming [9]. Whereas, in the case of DL, these models implement networked structures in order to mimic the human brain transforming imaging data in feature vectors.

Initially, DL models were towards image classification problems, then, object detection and finally, image segmentation, since the segmentation is seen as a pixel level classification problem where each pixel is classified with one of many label classes.

As an example, in the tumor segmentation process, each voxel can be classified as belonging to the class label of the object of interest or the background. Since it is a very common task across many problem domains, different DL based models have been developed for the delineation task including: fully convolutional [10], encoder-decoder [11], multi-scale and pyramid [12], attention [13], recurrent neural [14], generative and adversarial training [15] based networks.

The proposed methodology for this process could be henceforth as a first step the preprocessing phase that was based on an advanced de-noising technique. We used an anisotropic diffusion filter enriched by a normalization and a histogram equalization phase 'AHE' through Contrast Limited Adaptive Histogram Equalization 'CLAHE' method [10]. Such proposed preprocessing phase was consequently useful because the targeted segmentation process was considerably improved. The proposed segmentation technique of the MRI slices was based on a Deep Learning model referred to as Fully Connected Neural Network 'FCN' [16]. As an originality, this model was carefully modified by adding other residual connections in order to reinforce its efficiency. Such a modification reinforced the segmentation technique proved by the highest accuracy value around 98 %. Experimental results for various pathology cases represent a Computer Aided Diagnosis System that could be furnished to physicians during their exploring. Our proposed advanced MRI segmentation process could be extended towards a real clinical aided tool dedicated to clinical prostate exploration.

The main contribution of this research could be summarized as follows:

Our research involves at first a preprocessing phase that could be proposed for enhancing the segmentation process. Then, this advanced segmentation process itself would be useful for determining the ROI of the prostate and this would involve several main steps:

- A proposed modified FCN model would be inspired from the U-Net architecture.
- Adding skip connections to improve the performance of layers of this model
- Our proposed model was trained on Promise 12- Grand Challenge dataset
- CAD tool would be offered hence by this segmentation process dedicated to delineating the ROI for prostate.

The rest of this paper is organized as follows; section 2 explains our proposed method. In section 3 we present results and discussion and we compare our obtained results with the state-of-the-art. Section 4 present conclusion and perspectives.

II. PROPOSED METHOD

Figure 1 details our proposed methodology for MRI advanced segmentation dedicated to ROI prostate delineation. Such a computerized segmentation module would involve at the end a CAD system as a clinical aided tool.

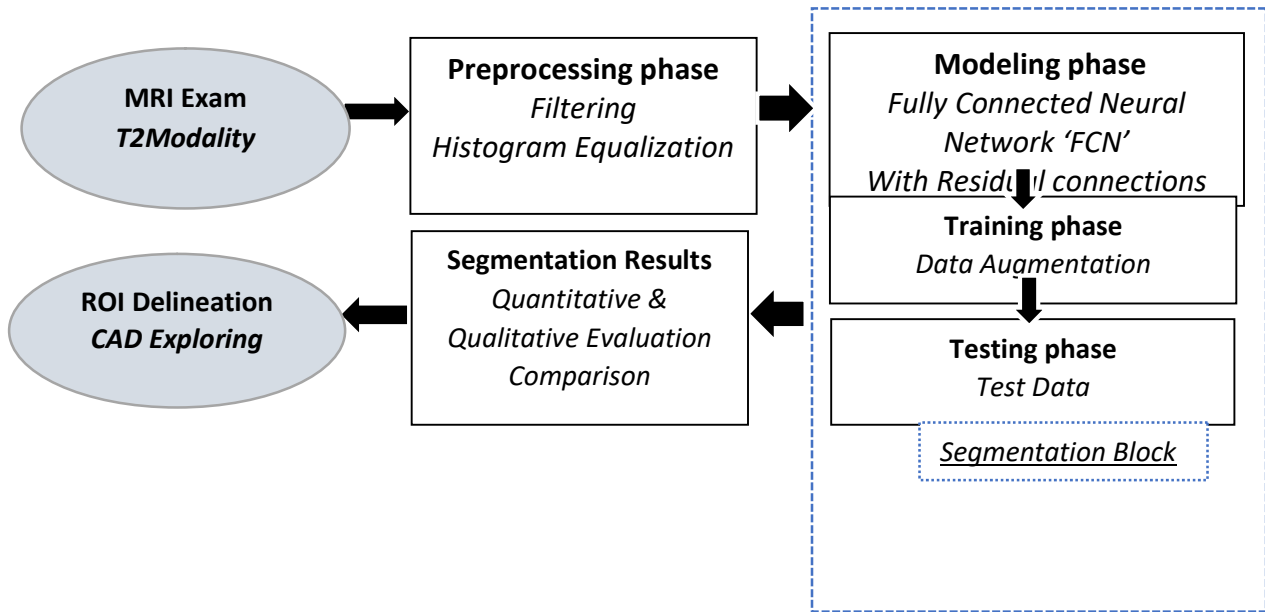


Figure1. Proposed strategy for advanced segmentation: ROI delineation for prostate clinical exploring

Preprocessing phase: *Towards the advanced segmentation process*

The main objective of preprocessing is the elimination of irrelevant information which facilitate the extraction of the useful information needed in the analysis. Several facts as sensor, sampling or body motion can affect MRI acquisition during the exam. The noise or artifact induces an effect that can be localized on a pixel. So, it is necessary to improve the quality of an image by enhancing the contrast. This phase is so important as it will reinforce our segmentation process.

The preprocessing protocol based on filtering in the first step, that was carefully studied when using one anisotropic filter [17] which will preserve all the clinical information and that is formulated as follows:

$$\partial_t u = \text{div}(g(<|\nabla_u|^2) \nabla_u) \tag{1}$$

$$\text{With } g(s^2) = \frac{1}{1+s^2/\lambda^2} \quad (\lambda > 0) \tag{2}$$

The choice of the anisotropic diffusion filter was proved after exploring several essential filters used for de-noising artifacts that could be present within MRI slices such as wavelet, median, Laplacian, gaussian wiener, nonlocal means filter..., we recommend this anisotropic filter that present interesting filtering results when avoiding blurring and localization faults. It is based on the nonlinear diffusion scheme [16]. This filter has the advantage of overcoming the faults of spatial filtering and remarkably increases the quality of the image. Also, it eliminates effectively the noise in uniform regions with sharp edges. We have proved in a previous study [16] the efficiency of Anisotropic filter (F_g) to denoise T2-Weighted MR images since its details preserving capability. We introduced the subjective assessment score F_g [17] that depends on human vision experience. Besides the usual measurement as Structural similarity index ‘SSIM’, Mean Squared Error ‘MSE’, Peak Signal to Noise Ratio ‘PSNR’ to compare filters efficiency. F_g is defined as follows:

$$F_g = \frac{\text{PSNR}_{/10+5}}{2} \tag{3}$$

Such as PSNR is $10 \log_{10}$ of the ratio of the maximum possible intensity value of an image to the square root of Mean Square Error (MSE) observed between the noisy and the original image.

$$PSNR = 10 \cdot \log_{10} \left(\frac{MAX_I}{\sqrt{MSE}} \right) \quad (4)$$

Advanced Segmentation Process

Our proposed advanced segmentation process is based on the following processing steps:

Modeling phase

Our model is inspired from U-Net architecture [15], which is an architecture originally used for semantic segmentation. The network consists of a contracting part and an expanding path, which gives it a "U" shaped architecture. The contracting part is a typical convolution network. It is based on the repeated application of convolutions, each followed by a rectified linear unit 'ReLU' and a maximum pooling operation. The expansive path combines geographic and spatial feature information through a sequence of upward convolutions and concatenations with high resolution features from the contracting path.

Fully Convolutional Neural Network 'FCN' has achieved great success in the application of dense pixel prediction in semantic segmentation. The algorithm is required for predicting a variable for all pixels of input image.

FCN is characterized by accepting input images at any size. It uses the deconvolution layer to up-sample the feature map of the last convolution layer and restore it to the same size of the input image. Thus, a prediction can be generated for each pixel. Finally, pixel-by-pixel classification is performed on the up-sampled feature map to complete the final image segmentation.

One of the major drawbacks of network down-sampling in an FCN is that it reduces the resolution of the input by a significant factor. Thus, when up-sampling, it is then very difficult to reproduce the finest details, even when using sophisticated techniques such as transposed convolution.

One way to overcome this is to add "skip connections" [6] in the up-sampling step from the previous layers and add the two feature maps together. These skip connections provide enough information to the subsequent layers to generate accurate segmentation boundaries. This combination of fine and coarse layers leads to local predictions with almost exact global (spatial) structure.

Adding Skip connections is considered as a Boosting method for an FCN. This operation improves the performance of layers by using predictions (feature maps) from previous layers.

Our FCN model has an encoder-decoder architecture. The encoder is usually a network (VGG, Resnet, Xception, etc); it consists of a deconvolution layer and upper sampling layer. Down sampling is intended to capture semantic or context information, while up sampling is intended to recover spatial information. Common decoders include bilinear interpolation, deconvolution, and dense up sampling convolution.

To summarize, adding skip connections helps reuse activations from the previous layer until the current layer learns its weights. It helps to update weights in a stable manner for smooth convergence of the network. In order to prevent the problem of overfitting, a dropout layer is added. Each residual block in the presented architecture consists of a 3x3 convolutional layer with a Rectified Linear Unit 'ReLU' layer as an activation function, a dropout layer, and another 3x3 convolutional layer with an ReLU layer as an activation function. We applied the same padding, unlike U-Net architecture, to keep output spatial dimensions, similar to the input feature map. The first convolution layer output is added with the next convolution layer output to form the residual connection in each block. In up-sampling, each layer consists of 2×2 kernel-sized blocks, similar to those used in down-sampling.

Training phase

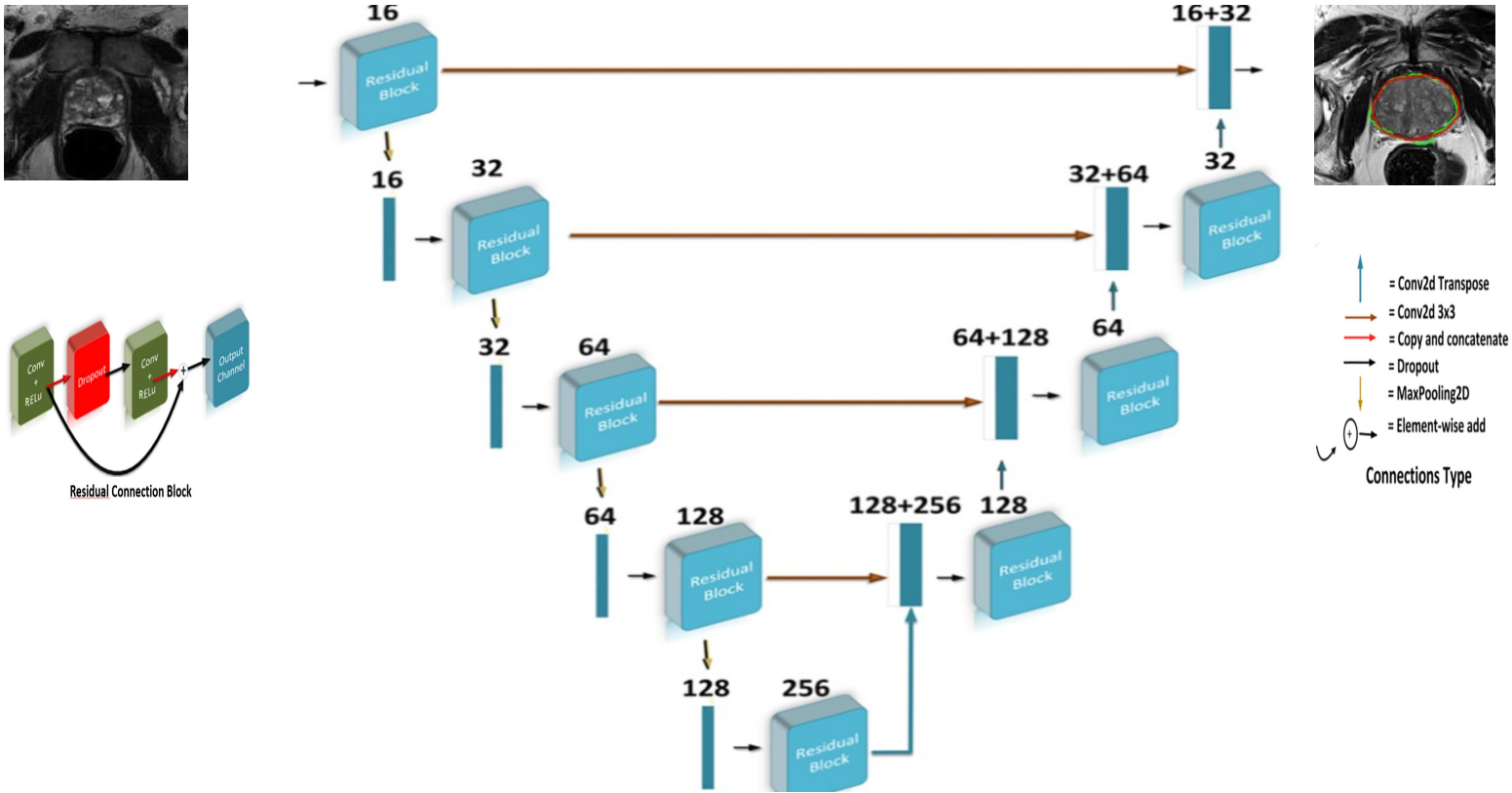
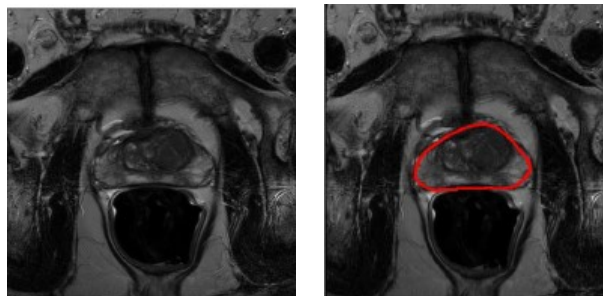


Figure2. Proposed modified FCN model by adding residual connections.
 Each arrow shows the individual operations performed.
 Each box shows the feature map.
 The number at the box top corresponds to channels' number

Our proposed model was tested on dataset downloaded from the PROMISE12-Challenge 'Prostate MR Image Segmentation'-challenge 2012. The dataset contains 49 patients for training with their labels given by expert radiologists, and 29 cases for testing. Images are in (.mhd and .raw) formats). Labels were performed under the supervision of expert radiologists to build ground-truth segmentation images used to evaluate the performance of our proposed model, as shown in figure 3 below. For each case, we have between 25 and 45 MRI slices. It contains in total about 1200 images for training our model.

Such a limited number of images generally leads to a model suffering from overfitting. To resolve this problem, we ought to increase the robustness and reduce overfitting, we employed henceforth the strategy of data augmentation to enlarge the training dataset. The data augmentation techniques include "scaling", "rotation", "flipping" and "elastic deformation".



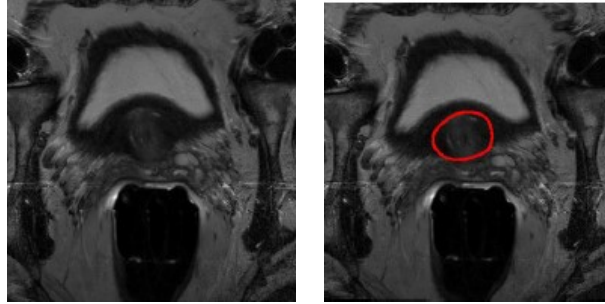


Figure3. Example of MRI slices from Promise 12- challenge dataset and its relative manual ground truth annotation

Figure 3 shows an example of MRI slices and labels. The red contour corresponds to the result of the superimposition of label in the original MRI slice.

Hyperparameters regroup the variables which determine the network structure as the Number of Hidden Units (are the layers between input layer output layer) and the variables which determine how the network is trained as the Learning Rate. In our implementation, we fixed the following parameters; Dropout as regularization technique, ReLU as activation function, Adam as optimizer, learning rate=0.001, batch size= 16 and finally Number of epochs= 15.

Testing phase

The proposed algorithm for prostate segmentation was evaluated on 4640 MRI slices from Promise-12_Challenge dataset.

We used quantitative measurements to estimate the performance of the proposed FCN architecture.

The performance evaluation measurements are referred to Promise 12_challenge[19] as Volumetric Dice similarity ‘DSC’, Mean Relative Absolute Volume ‘RAV’, Mean Surface distance ‘MSD’ and Hausdorff Distance ‘HD’.

- **Volumetric Dice Similarity:** is used for the efficiency evaluation of our model. It describes the manner of the model’s predicted mask superimposes with the ground-truth mask. Matimatically, it is defined as:

$$Dice\ coefficient = \frac{2*TP}{(TP+FP)+(TP+FN)} \quad (1)$$

With TP: the true positive

FP: false positive

FN: false negative

- **Mean Surface Distance (MSD):** Corresponds to how much, on average, the surface varies between the segmentation and the ground truth (in mm).

$$MSD = \frac{1}{n_g+n'_g} (\sum_{p=1}^{n_g} d(p, S') + \sum_{p'=1}^{n'_g} d(p', S)) \quad (2)$$

- **Hausdorff Distance (HD)** - the maximum of the vector. The largest difference between the surface distances. Also measured in mm. We calculate the *symmetric Hausdorff distance* as:

$$HD = \max [d(S, S'), d(S', S)] \quad (3)$$

- **Accuracy:**

$$Accuracy = \frac{TP}{TP+TN} * 100 \quad (4)$$

III. RESULTS AND DISCUSSION

Preprocessing Results

To denoise MRI slices, we’ve tested different filters as wavelet, median, Laplacian, gaussian, etc. we ‘ve used several evaluation metrics as PSNR, MSE, SSIM. We ‘ve added subjective (qualitative) measurement that is the

most reliable judgment in assessing image quality. It is performed by humanobservers. The final score F_s is computed finally to regroup subjective and objective assessment.

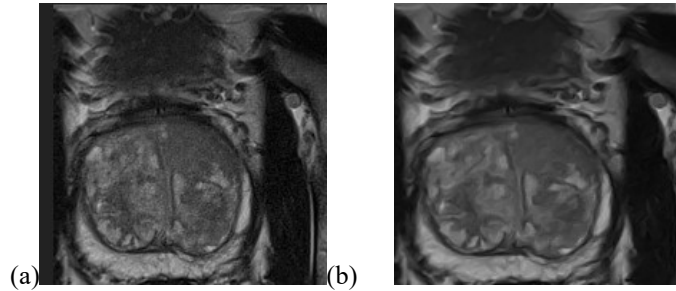


Figure 4. Result of denoised image using the anisotropic diffusion filter
(a) Original image, (b) Filtered image

Through our comparison, we ‘ve concluded that the anisotropic filter is the best for denoising MRI slices. This filtering process would be persuaded by a Histogram Equalization technique referred to us CLAHE (Contrast Limited Adaptive Histogram Equalization). This was another means of enhancing the contrast of the different MRI slices which would be so useful for the efficiency of the targeted segmentation process. Therefore, interesting results were tested and we can give an example in the following figure:

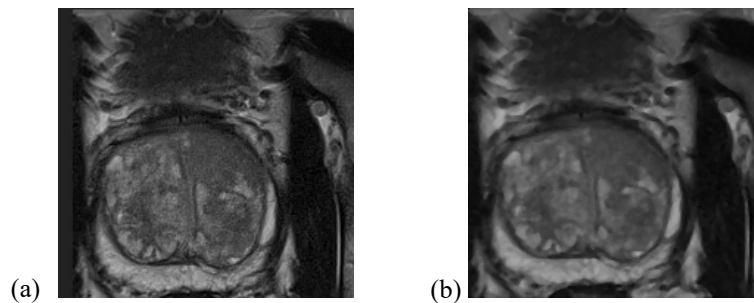


Figure 5. Histogram equalization using CLAHE technique
(a) Original image, (b) Equalized image

Table 1 shows the results before and after applying preprocessing steps. The performance of our proposed method increased after preprocessing.

Table 1. Results before and after preprocessing

Preprocessing	Dice Coefficient (%)	Accuracy (%)
Before	81.52	89.12
After	95.10	98.01

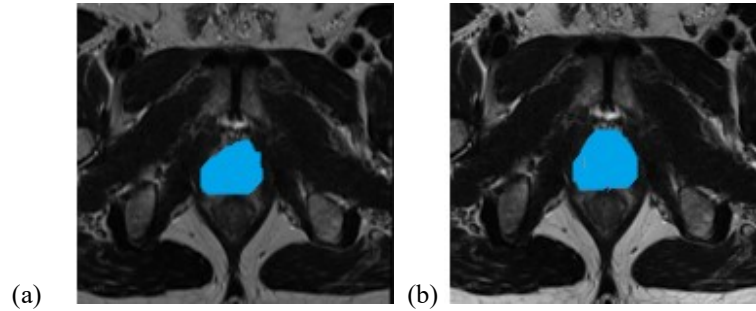


Figure 6. Preprocessing effect on segmentation process
 (a) Segmentation without preprocessing (b) Segmentation with preprocessing

Advanced Segmentation Results

The prostate structure has fuzzy boundaries and the pixel intensity distributions are inhomogeneous both inside and outside the prostate. Therefore, both prostate and non-prostate regions have similar contrast and intensity distributions. All of these factors make the segmentation as a difficult challenge to overcome.

The advanced segmentation results as presented in this paper could be summarized as follows: we present at first an essential step illustrating the qualitative evaluation to be continued by a quantitative evaluation enriched by a brief comparison with the state of the art.

Clinicians would need essentially the qualitative evaluation that could be enriched later by essential quantitative parameters that could have an impact clinically.

Our proposed computerized tool which was capable of helping clinicians during their exploring by delineating precisely the prostate ROI regions could be furnished via a more convivial software reassembling the different modules. Such a research work could constitute henceforth one CAD system that could be offered for prostate exploring.

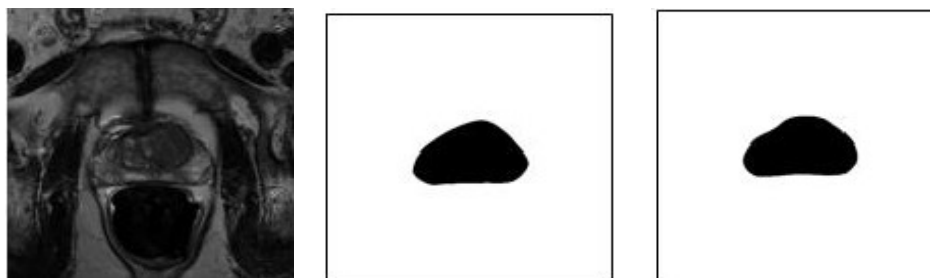
Qualitative Evaluation

As we performed slice-by-slice advanced segmentation that focuses on delineating the prostate ROI regions for clinical needs, qualitative results depicted by visualization mainly were presented.

Qualitative evaluation as presented in this section could be in two stages: the first stage would involve the prostate ROI extraction including comparison with Radiologist manual ROI extraction.

The second stage would involve more efficiently ROI prostate delineation including also comparison with Radiologist manual delineation.

Figure 7 as presented below was illustrated by three columns relatively to four patients. Column (a) depicted the T2-w MRI selected slice. Column (b) depicted the ROI Radiologist manual extraction at first where column (c) depicted the ROI advanced segmentation extraction. This automated prostate ROI extraction was in fact in concordance with the used ground truth. Such a needed module could be integrated as a first stage proposed for the Computer Aided Diagnosis useful for automating ROI prostate exploring to be used later by clinicians.



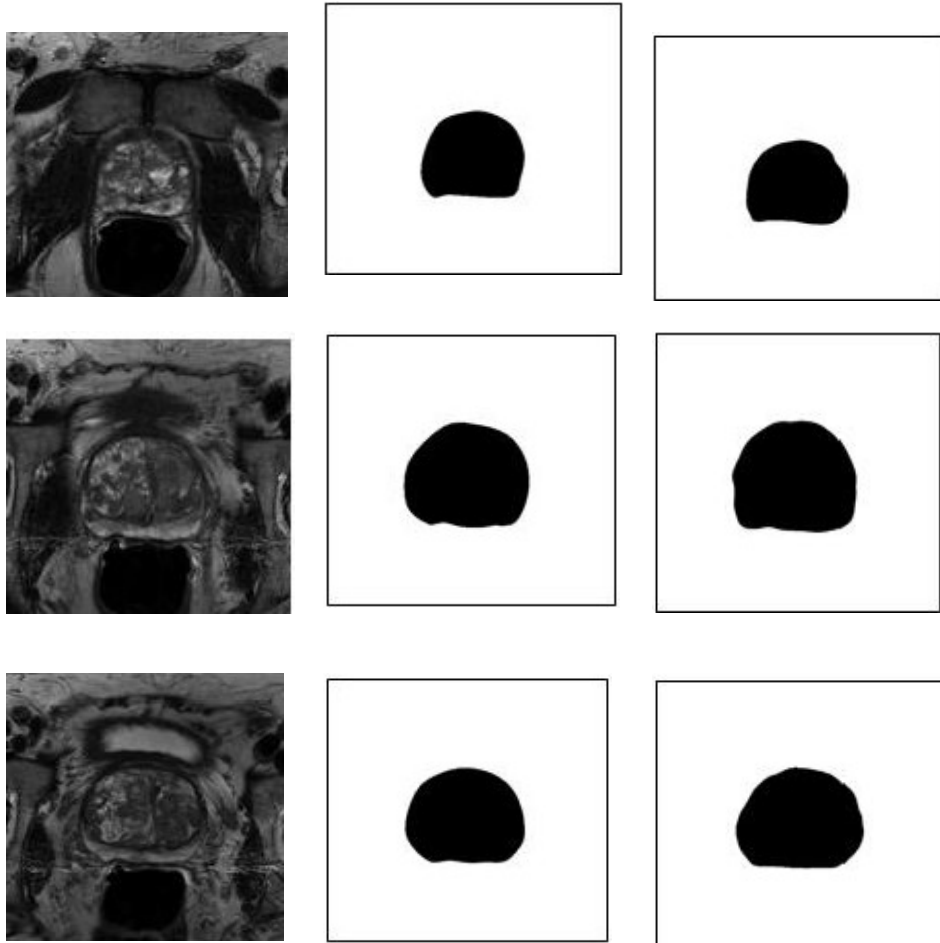
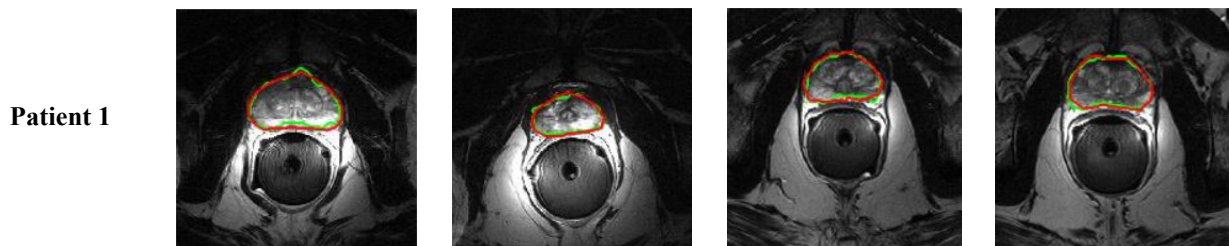


Figure 7. ROI extraction results from T2-w MRI selected slices
 (a) ROI Radiologist manual extraction (b) ROI advanced segmentation extraction
 Towards Computer Aided Diagnosis for ROI prostate exploring

Figure 8 as presented below was illustrated by four columns relatively to four patients. These pathological patients were chosen arbitrarily from the dataset and four T2-w MRI slices were selected for each. Results' delineation was highlighted in Green and Radiologist manual delineation was highlighted in Red. This automated prostate ROI delineation was in fact in concordance with the used ground truth. Such a needed module could be integrated also as a second and essential stage proposed for the Computer Aided Diagnosis tool. This tool would be so useful for automating ROI prostate exploring to be used later by clinicians.



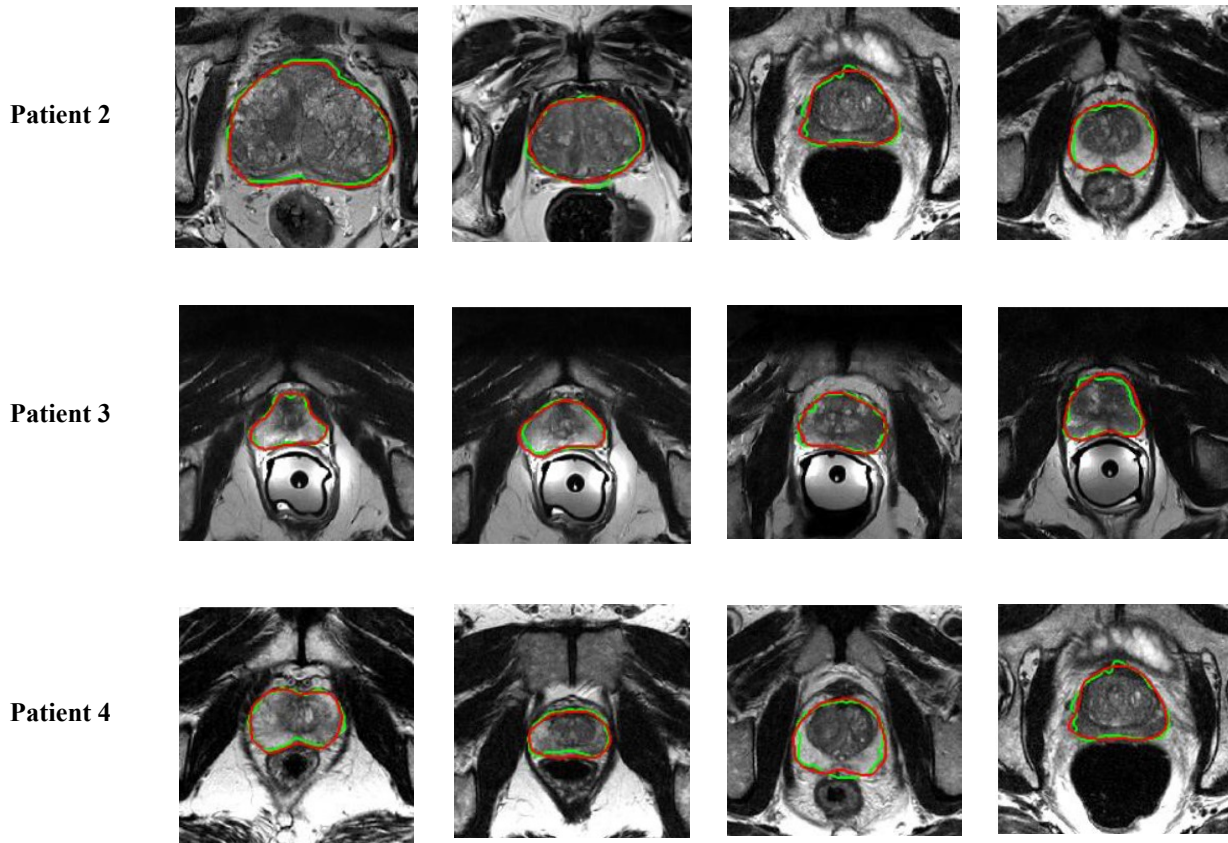


Figure 8. Advanced segmentation results based on proposed modified FCN model
Four pathological patients, Four T2-w MRI selected slices
Results' delineation highlighted in Green and Radiologist manual delineation in Red
Towards Computer Aided Diagnosis for ROI prostate exploring

Quantitative Evaluation

The proposed algorithm as for an advanced prostate segmentation was quantitatively evaluated on 4640 T2-w MRI slices issued from Promise-12 Challenge dataset.

We used quantitative measures to estimate the performance of the proposed modified FCN architecture.

Table 2 shows the performance of the proposed modified FCN model with residual connection in terms of accuracy and Dice metric in comparison with some other studies from the state-of-the-art. These studies used the same Promise-12-dataset.

Table 2. Comparison results of our proposed method with the state-of-the-art

Authors	Accuracy (%)	Dice (%)	Method description
A. LatrAch& al.	<u>98.01</u>	<u>95.10</u>	FCN with residual connections
Tian & al. [10]	91.5	85.3	Long FCN model
Ghassab& al. [8]	94	87	Active Appearance Model
Cho et al. [7]		78	CNN with topological derivative
Hossain et al. [6]		94.57	VGG 19 Rseg
Zhu at al. [5]		88.5	Deeply Supervised CNN

As shown in the previous table, our proposed modified FCN model has the higher accuracy and better Dice metric comparing with the other similar methods. We depict hence the effectiveness of the residual connections in the network over conventional series connections.

Regarding the next best case in Table 2 which is the VGG 19 Rseg by [6], one could remark that this model used only basic preprocessing such as normalization of pixel values.

In the deeply supervised CNN [5], additional deeply supervised layers were introduced to improve the detection of prostate region. It was found that in deep convolutional networks, pixel information was lost and this could explain the achieved result which was 88.5%.

The Active Appearance model presented a partial contour-based segmentation method utilizing an a priori shape [8]. These methods rely greatly on identifying suitable feature information.

The CNN with topological derivative [7] failed to obtain satisfactory results over other similar methods. The model could detect only one part of the overall prostate region. However, for the details of prostate, for instance, the boundaries, the network cannot assign the label to each pixel accurately.

IV. CONCLUSION

This research concerned the development of CAD system based on an advanced segmentation technique dedicated to extract and delineate the ROI of the prostate. Our proposed methodology involved as a first step the preprocessing phase by investigating an advanced de-noising technique using an anisotropic diffusion filter with a normalization and a histogram equalization phase through Contrast Limited Adaptive Histogram Equalization method. Such proposed preprocessing phase was consequently useful because the targeted segmentation process was considerably improved.

The segmentation technique of the MRI slices used a Deep Learning model referred to as Fully Connected Neural Network 'FCN'. As an originality, this model was carefully modified by adding other residual connections in order to reinforce its efficiency. Such an added modification reinforced in fact the segmentation technique allowing consequently the highest accuracy value around 98 %.

These advanced segmentation results were promising and useful clinically especially when they were discussed largely with clinical staff. Various pathological cases were carefully experimented and results are promising and encouraging for continuing this process. This could involve a useful CAD System that would be furnished to physicians during their clinical prostate exploring. Our perspective behind this proposed advanced MRI segmentation process could be extended henceforth towards a real aided tool dedicated to clinical prostate exploration.

REFERENCES

- [1] Trigui, R.; *Dépistage et classification du cancer de la prostate par la fusion des données SRM et IRM*; defended thesis (doctorate degree) at University of Dijon, France with ATMS Lab of Tunisia; 2017.
- [2] Trigui, R.; Miteran, J.; Walker, P.M.; Sellemi, L.; Ben Hamida, A.; *Automatic classification and localization of prostate cancer using multi-parametric MRI/MRS*; *Biomedical Signal Processing and Control*, ELSEVIER; vol31; Pages 189-198; 2017.
- [3] He, J.; Deng, Z.; Qiao, Y.; *Dynamic multi-scale filters for semantic segmentation*; In Proceedings of the IEEE International Conference on Computer Vision; Seoul, Korea; 27 October–2 November 2019.
- [4] Chen, L.C.; Yang, Y.; Wang, J.; Xu, W.; Yuille, A.L.; *Attention to Scale: Scale-Aware Semantic Image Segmentation*; In Proceedings of the IEEE Computer Society Conference on Computer Vision and Pattern Recognition; Las Vegas, NV, USA; 2016.
- [5] Zhu Y.; Williams S.; Zwiggelaar R.; *Segmentation of volumetric prostate MRI data using hybrid 2D + 3D shape modeling*; In Proceedings of medical image understanding and analysis; pp 61–64; 2004.
- [6] Sazzad, Md.H.; Paplinski, Andrew. P.; Betts, John. M.; *Residual Semantic Segmentation of the Prostate from Magnetic Resonance Images*; Faculty of Information Technology, Monash University, Melbourne, Australia; Springer Nature Switzerland AG; 2018.
- [7] Cho, C.; Lee, Y.H.; Lee, S.; *Prostate detection and segmentation based on convolutional neural network and topological derivative*; In proceedings of the 2017 IEEE International Conference on Image Processing (ICIP); Beijing; pp4452–4456; 2017.
- [8] Ghasab, M.A.J.; Paplinski, A.P.; Betts, J.M.; Reynolds, H.M.; Haworth, A.; *Automatic 3D modelling for prostate cancer brachytherapy*; In proceedings of the 2017 IEEE International Conference on Image Processing (ICIP); Beijing; pp 4452–4456; 2017.
- [9] Cuocolo, R.; Cipullo, M.B.; Stanzione, A.; Ugga, L.; Romeo, V.; Radice, L.; Brunetti, A.; Imbriaco, M.; *Machine learning applications in prostate cancer magnetic resonance imaging*; *European. Radiology Journal*; pp3, 35; Exp. 2019.
- [10] Tian, Z.; Liu, L.; Fei, B.; *Deep convolutional neural network for prostate MR segmentation*; In proceedings of the Medical Imaging 2017: Image-Guided Procedures, Robotic Interventions, and Modeling; International Society for Optics and Photonics; vol. 10135; p. 101351L; 2017.
- [11] Jia, H.; Xia, Y.; Song, Y.; Cai, W.; Fulham, M.; Feng, DD.; *Prostate segmentation in MR images using ensemble deep convolutional neural networks*; *IEEE International Symp Biomed Imaging* 762–765; [https:// doi.org/ 10. 1109/ isbi. 2017. 79506 30](https://doi.org/10.1109/isbi.2017.7950630); 2017.

- [12] Long, J.; Shelhamer, E.; Darrell, T.; *Fully convolutional networks for semantic segmentation*; In Proceedings of the IEEE Computer Society Conference on Computer Vision and Pattern Recognition; Boston, MA, USA; 7–12 June 2015.
- [13] Vincent, P.; Larochelle, H.; Lajoie, I.; Bengio, Y.; Manzagol, P.A.; *Stacked denoising autoencoders: Learning Useful Representations in a Deep Network with a Local Denoising Criterion*; Journal of Machine Learning Research; 11, 3371–3408; 2010.
- [14] Zhao, H.; Shi, J.; Qi, X.; Wang, X.; Jia, J.; *Pyramid scene parsing network*; In Proceedings of the 30th IEEE Conference on Computer Vision and Pattern Recognition, CVPR 2017; Honolulu, HI, USA; 21–26 July 2017.
- [15] Radford, A.; Metz, L.; Chintala, S.; *Unsupervised representation learning with deepconvolutional generative adversarial networks*. In Proceedings of the 4th International Conference on Learning Representations, ICLR 2016—Conference Track Proceedings; San Juan, Puerto Rico; 2–4 May 2016.
- [16] Mirza, M.; Osindero, S.; *Conditional Generative Adversarial Nets Mehdi*; arXiv 2018, arXiv:1411.1784; 2018.
- [17] Latrach, A.; Trigui, R.; Sellemi, L., *Denoising techniques for multi-parametric prostate MRI: A Comparative Study*; [International Conference on Advanced Technologies for Signal and Image Processing](https://doi.org/10.1109/ATSIP49331.2020.9231751) ATSIP 2020; <https://doi.org/10.1109/ATSIP49331.2020.9231751>; 2020.
- [18] Gaurav, G.; Mamta, J.; *A survey of denoising techniques for multi-parametric prostate MRI*; Multimedia Tools and Applications; <https://doi.org/10.1007/s11042-018-6487-; 2019>.
- [19] MICCAI Grand Challenge: Prostate MR Image Segmentation 2012. <https://promise12.grand-challenge.org/>